VISIT: Placement of Unmanned Aerial Vehicles for Anisotropic Monitoring Tasks

Weijun Wang* Haipeng Dai* Chao Dong† Fu Xiao‡ Xiao Cheng* Guihai Chen*
*State Key Laboratory for Novel Software Technology, Nanjing University, Nanjing, Jiangsu 210024, CHINA
†Nanjing University of Aeronautics and Astronautics, Nanjing, Jiangsu 210007, CHINA
‡Nanjing University of Post and Telecommunication, Nanjing, Jiangsu, China
Emails: {weijunwang, xiaocheng}@nju.edu.cn, dch999@gmail.com, {haipengdai, gchen}@nju.edu.cn, xiaof@njupt.edu.cn

***Abstract*—This paper considers the fundamental problem of placement of Unmanned Aerial VehIcles for aniSotropic monItoring Tasks (VISIT). That is, given a set of objects on 2D area, place a fixed number of UAVs by adjusting their coordinates and orientations subject to Gaussian bias, such that the overall monitoring utility for all objects is maximized. We develop a theoretical framework to address VISIT. First, we establish the monitoring model whose quality of monitoring (QoM) is anisotropy with respect to monitoring angle and monitoring distance. To the best of our knowledge, we are the first to consider anisotropic QoM. Then, we propose an algorithm consisting of area discretization and Monitoring Dominating Set (MDS) extraction, to reduce the infinite solution space to a limited one without performance loss. Finally, we prove that the reformulated problem can be modeled as maximizing a monotone submodular function subject to a matroid constraint and present a greedy algorithm with $1-1/e-\epsilon$ approximation ratio to address it. We conduct both simulations and field experiments to evaluate our algorithm, and the results show that our algorithm outperforms comparison algorithms by at least 41.3%.**

I. Introduction

Camera sensor networks have attracted great attention in recent years as they provide detailed data of environments by retrieving rich information in the form of images and videos [1]. The application range of camera sensor networks is wide, such as surveillance, traffic monitoring, and crowd protection. For some temporary situations, such as assembly, concerts, and outdoor speeches, establishing stationary camera sensor networks in advance may cost too much time and money, and may be inconvenient or even impossible. Fortunately, development of Unmanned Aerial Vehicle (UAV) technology in the past few years [2]–[4] offers a promising way to address this issue. With low-cost and agile UAVs, camera sensor networks can be deployed dynamically to provide real-time, reliable, and high-quality images and videos. For example, *DJI Phantom 4* UAV can fly at $72\,km/h$, rise at $6\,m/s$, swerve at $250\,^\circ/s$, and provide $2K$ real-time images and videos [5].

To obtain better monitoring performance, UAVs should adjust their coordinates and orientations (the combinations of which are defined as *strategies*) to monitor frontal view of objects [6], because figures from this view provide key information in applications such as face recognition and vehicle license plate recognition. We assume that the UAV flies horizontally at the same altitude and define the Quality of Monitoring (QoM) to measure the monitoring quality of an object by a UAV. As shown in Figure 1, an object o_j can be *efficiently monitored* (defined in Section III) by a UAV u_i when o_j is located in the monitored region around the orientation $\vec{d}_{ui}$ of u_i, and u_i is located in the region near the frontal view $\vec{d}_{oj}$ of o_j. Moreover, QoM is anisotropic and continuous as shown in Figure 2. With the increase of the distance between object and UAV or the increase of the angle between the orientation of an object and the vector coming out from it to UAV, QoM decreases monotonically [7]. For example, in Figure 1, u_1 provides better QoM than u_2.

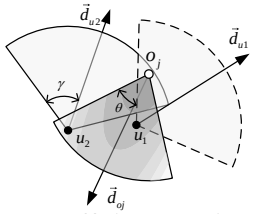

Fig. 1: Efficient monitoring model

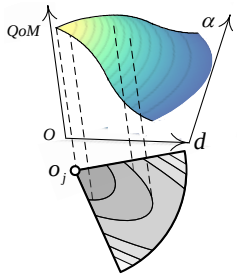

Fig. 2: Anisotropic QoM Model

Moreover, multiple monitoring images of different strategies can be jointly exploited to achieve better monitoring performance. For example, in computer vision, utilizing different images of objects from multiple views has been proved to be able to dramatically improve the recognition accuracy than only from one view [6]. Thus, we define *monitoring utility* to characterize the quality of monitoring for one object monitored from multiple views. However, due to practical factors, *e.g.*, limited accuracy of GPS, the bias of orientation, the influence of wind, and noise over the channel for image transmission [8], the captured images are biased. To this end, we use Gaussian distribution to model the aggregate effect of these factors, which is widely used in existing literature (*e.g.*, [9], [10]).

In this paper, we study the problem of placement of Unmanned Aerial VehIcles for aniSotropic monItoring Tasks (VISIT). Formally, given a set of objects with known coordinates and directions on the plane, the VISIT problem is to deploy a fixed number of UAVs (*i.e.*, to determine their strategies) by considering the Gaussian bias such that the overall monitoring utility for all objects is maximized.

In previous works, there have emerged methods studying

efficient monitoring problem [11]–[16], but none of them can address our problem as they simply consider an object being either covered or not, not the more practical QoM model as considered in this paper. Some other methods adopt QoM model (*e.g.*, [17]–[22]), but most of them assume omnidirectional models for both sensors and objects, while the others neglect the anisotropy of QoM, which makes them not suitable for our problem. In summary, none of the existing works can be utilized to solve the considered problem in this paper.

To address the VISIT problem, we face three main technical challenges. First, the aggregate effect of practical factors, which can be modeled as Gaussian distribution, is difficult to deal with in theoretical analysis. Second, for each UAV, the solution space of its strategy, which includes coordinate and orientation, is infinite and continuous. Third, the problem is NP-hard, thus we need to develop an approximation algorithm with performance guarantee.

To address the first challenge, we introduce the entropy of Gaussian random variable into our monitoring utility model and establish conditional covariance matrix to quantify the monitoring utility with reduction of variance. To address the second challenge, we first approximate the nonlinear QoM function as piecewise constant to make the objective function almost linear. Then, we propose a Monitoring Dominating Set (MDS) extraction method to reduce the continuous search space of strategies of UAVs to a limited one without performance loss. Hence, the VISIT problem becomes selecting a fixed number of strategies from a set of candidate ones to maximize the overall monitoring utility, which is discrete. To address the third challenge, we prove that the reformulated problem falls into the scope of the problem of maximizing a monotone submodular function subject to a matroid constraint, which allows a greedy algorithm to achieve a constant approximation ratio.

We conducted both simulations and field experiments to evaluate our algorithm. The results show that our algorithm outperforms comparison algorithms by at least 41.3%.

II. Related Work

Some camera placement methods consider the direction of objects [11]–[16]. [11] proposes the full-view coverage model by introducing objects' facing direction into coverage model. [12] proposes an effective dalgorithm to solve full-view coverage problem in the mobile heterogeneous camera sensor networks. [13]–[15] all focus on barrier coverage with minimum number of sensors. But most of them do not consider the QoM in their adopted sector coverage model.

Some camera placement methods consider the QoM in their sensing region [17]–[19]. [17] utilizes a signal propagation model to quantify the QoM, and proposes algorithms to minimize ratio of false alarm and maximize ratio of alarm. [18] proposes a fusion model to fuse the sensing value as QoM and utilizes this fusion model to design an algorithm to minimize number of sensors. [19] considers the energy consumption of sensors and combines fusion model to propose energy-efficient algorithm. But most of them do not consider objects' direction.

TABLE I: Notations

Symbol	Meaning
u_i	UAV i, or its coordinate
o_j	Object j to be monitored, or its coordinate
$\mathcal{U}$	Set of all UAVs
$\mathcal{O}$	Set of all objects
M	Number of UAVs to be deployed
N	Number of objects to be monitored
$\vec{d}_{ui}$	Orientation of UAV i
s_k	Strategy k $\langle u_i, \vec{d}_{ui}\rangle$ of UAV i with orientation $\vec{d}_{ui}$
A_l	Subarea l formed by a set of discretized sectors of O_l
$\mathcal{S}$	Set of selected strategies
γ	Monitoring angle of the field of view (FoV) around $\vec{d}_{ui}$
$\vec{d}_{oj}$	Orientation of object o_j
θ	Efficient angle around $\vec{d}_{oj}$ for efficient monitoring
d_{min}	Minimum distance between UAV and object for safe
D	Monitoring distance of FoV of camera of UAV
ω	Key information in ω angle around object
β	Distribution angle of key information of object

A few camera placement methods consider both QoM and direction of objects [20]–[22]. [20] considers the weighted sensing quality and the importance of sensing area. [21] considers the size of objects and proposed an algorithm to minimize the number of cameras as well as avoid occlusion. [22] qualifies the coverage QoM as k-barrier and studied jointly deploying minimum number of mobile and stationary directional sensors to achieve k-barrier coverage. However, none of them consider the anisotropic QoM in coverage area.

III. Problem Formulation

A. Efficient Monitoring Model

Suppose we have N objects $\mathcal{O} = \{o_1, o_2, ..., o_N\}$ distributed on a 2D plane Ω with fixed coordinates o_j and orientations $\vec{d}_{oj}$, and M UAVs $\mathcal{U} = \{u_1, u_2, ..., u_M\}$ equipped with cameras can be placed anywhere on Ω with any orientation. The tuple $\langle u_i, \vec{d}_{ui}\rangle$, called $strategy$, where u_i denotes the coordinate of UAV i and $\vec{d}_{ui}$ denotes its orientation. By a little abuse of notation, u_i and o_j also denotes UAV i and object j. Table I lists the notations we used in this paper.

***Definition** 3.1:* **(Efficient monitoring)** An object o_j is efficiently monitored if for a given vector $\vec{d}(x, y)$ (its facing direction), there is a UAV u_i, such that o_j is monitored by u_i and $\alpha(\vec{d}, \overrightarrow{o_j u_i}) \leq \theta$ (θ is called the effective angle).

Based on Definition 3.1 and assuming that the UAV flies horizontally at the same altitude, the efficient monitoring model can be modeled as a sector like in [13]–[15]. A UAV u_i with orientation $\vec{d}_{ui}$ monitors objects with non-zero QoM in a *monitoring area* of a sector with *monitoring angle* γ and radius D. An object o_j with orientation $\vec{d}_{oj}$ can be efficiently monitored with non-zero QoM in a *monitored area* of a sector with *efficient angle* θ and the same D. Figure 1 illustrates two pairs of efficient monitoring, u_1 with o_j and u_2 with o_j.

To achieve high QoM, UAVs need to capture high-resolution images of objects. Image resolution is the ratio of the number of pixels and the image size, whose unit is Pixels Per Inch (PPI). Thus, the number of pixels in the image is nearly square

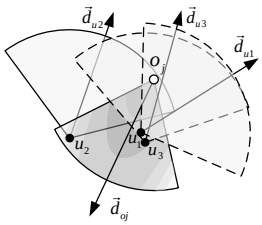

Fig. 3: Efficient monitoring model

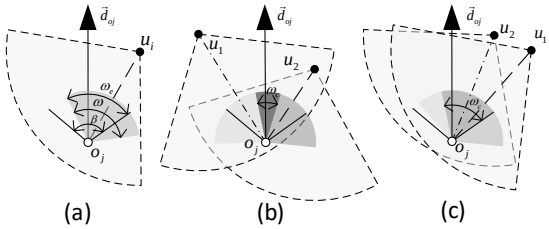

Fig. 4: Fusion model

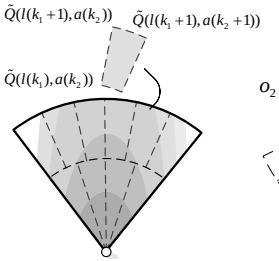

Fig. 5: Approximation illustration

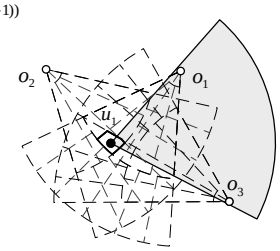

Fig. 6: Area discretization

of the distance between objects and UAVs [7]. The QoM is also anisotropic. With the monitoring angle $\alpha(\vec{d}_{oj}, \overrightarrow{o_j c_i})$ increasing, the number of pixels of the frontal view of object is also decreasing. Therefore, the QoM of efficient monitoring pair u_i and o_j can be modeled as follows:

$$\mathcal{Q}(u_i, o_j, \vec{d}_{ui}, \vec{d}_{oj}) = \begin{cases} \frac{a}{(||u_i o_j||+b)^2}\cos(\alpha(\vec{d}_{oj}, \overrightarrow{o_j u_i})), 0 \le ||u_i o_j|| \le D, \\ \qquad\qquad \overrightarrow{u_i o_j}\cdot\vec{d}_{ui} - \|u_i o_j\|\cos\gamma \ge 0, \\ \qquad and \quad \overrightarrow{o_j u_i}\cdot\vec{d}_{oj} - \|o_j s_i\|\cos\theta \ge 0. \\ 0, \qquad\qquad otherwise. \end{cases} \tag{1}$$

where a and b are two constants determined by the surrounding environment and the hardware of UAVs, $||u_i o_j||$ is the distance between u_i and o_j, and $\alpha(\vec{d}_{oj}, \overrightarrow{o_j u_i})$ is the included angle between $\vec{d}_{oj}$ and $\overrightarrow{o_j u_i}$. Note that here $\cos(\cdot)$ function is used only for simplicity, other functions conforming to the decreasing along with angle characteristic can also work well.

B. Monitoring Utility

1) Fusion Function: Multiple images from different views of an object can provide different information, which contributes to better monitoring performance. However, information fusion is not trivial linear addition because monitoring images of an object from nearby strategies are often highly correlated. As shown in Figure 3, images captured by $\langle u_1, \vec{d}_{u1}\rangle$ and $\langle u_3, \vec{d}_{u3}\rangle$ both monitor the left side of o_j with similar efficient angle, while $\langle u_2, \vec{d}_{u2}\rangle$ monitors the right side. Thus, $\langle u_1, \vec{d}_{u1}\rangle$ is highly correlated with $\langle u_3, \vec{d}_{u3}\rangle$ but not with $\langle u_2, \vec{d}_{u2}\rangle$. Although $\langle u_3, \vec{d}_{u3}\rangle$ provides better QoM of o_j than $\langle u_2, \vec{d}_{u2}\rangle$, placing UAVs at $\langle u_1, \vec{d}_{u1}\rangle$ and $\langle u_2, \vec{d}_{u2}\rangle$ can provide more information than at $\langle u_1, \vec{d}_{u1}\rangle$ and $\langle u_3, \vec{d}_{u3}\rangle$. Thus, we need to quantify the correlation of multiple strategies.

Here, we use the amount of common information of multiple strategies to quantify their correlation. Figure 4(a) illustrates the key information distribution and extraction region for an object. The key information distributes in the region of β angle around the frontal view of o_j. Each u_i can capture ω angle region of information distributed around o_j, but only $\omega \cap \beta$ region captures key information, saying ω_e. In Figure 4(b) and 4(c), both u_1 and u_2 monitor ω angle of o_j, but the common monitoring angle ω_c is different. The common monitoring angle ω_c in Figure 4(b) is smaller than that in Figure 4(c), thus the strategies of u_1 and u_2 in Figure 4(c) are more correlated. The correlation can be quantified with $\frac{\omega_c}{\beta}$. In general case, a UAV can monitor a set of objects in one image. Suppose u_i monitors a set of objects $\mathcal{O}_i$ and u_j monitors $\mathcal{O}_j$, $\mathcal{O}_i \cap \mathcal{O}_j = \mathcal{O}_k$ Then, the correlation model is given by

$$\begin{aligned} \mathcal{K}(u_i, u_j, \vec{d}_{ui}, \vec{d}_{uj}, \mathcal{O}_k) =& \frac{1}{(|\mathcal{O}_i| + |\mathcal{O}_j|)\beta}\sum_{k=1}^{|\mathcal{O}_k|}\int_{\vec{d}_{ok}-\frac{\beta}{2}}^{\vec{d}_{ok}+\frac{\beta}{2}} \omega_c d(\vec{v}) \\ =& \frac{1}{(|\mathcal{O}_i| + |\mathcal{O}_j|)\beta}\sum_{k=1}^{|\mathcal{O}_k|}(\omega - \alpha(\overrightarrow{o_k u_i}, \overrightarrow{o_k u_j})), \\ s.t. \quad & \mathcal{Q}(u_i, o_k, \vec{d}_{ui}, \vec{d}_{ok}) \neq 0, \mathcal{Q}(u_j, o_k, \vec{d}_{uj}, \vec{d}_{ok}) \neq 0, \end{aligned} \tag{2}$$

where $|\mathcal{O}_k|$ is the size of $\mathcal{O}_k$ and $\vec{v}$ is the angle variable changing from $\vec{d}_{ok} - \frac{\beta}{2}$ to $\vec{d}_{ok} + \frac{\beta}{2}$. If there exists no same object monitored by u_i and u_j, their correlation $\mathcal{K}(\cdot) = 0$.

2) Variance Reduction: Different sets of strategies provide different information of objects. The more different high-quality information is captured, the better monitoring performance can be obtained. So we should better monitor each object with higher QoM as well as lower correlation of key information.

We adopt the technique of *variance reduction* [23], [24] to analyze QoM correlation. Different strategies provide different reductions in the variance of recognition accuracy. The higher reduction of variance, the higher monitoring performance can obtain. Moreover, according to the probability theory, given a fixed covariance matrix, conditional covariance is independent to the actual observed values $\mathcal{A}$. This theorem motivates us to place UAVs in advance.

Due to practical factors such as limited accuracy of GPS, bias of orientation, and influence of wind in the air, the captured images are biased. We use Gaussian distribution to model the aggregate effect of these factors. The entropy of a Gaussian random variable y conditioned on a set of Gaussian random variables $\mathcal{A}$ can be expressed as [25]

$$H(y|\mathcal{A}) = \frac{1}{2}log((2\pi e)\sigma^2_{y|\mathcal{A}}). \tag{3}$$

Hence, it only depends on the covariance $\sigma^2_{y|\mathcal{A}}$, and the conditional covariance is given by:

$$\sigma^2_{y|\mathcal{A}} = \sigma^2_s - \Sigma_{y\mathcal{A}}\Sigma^{-1}_{\mathcal{A}\mathcal{A}}\Sigma_{\mathcal{A}y}, \tag{4}$$

where $\Sigma_{\mathcal{A}\mathcal{A}}$ is the covariance matrix of $\mathcal{A}$ with itself and $\Sigma_{y\mathcal{A}} = \Sigma^T_{\mathcal{A}y}$ is a row vector of the covariances of y with all variables in $\mathcal{A}$.

We can establish the kernel matrix as $\Sigma = \begin{pmatrix} \Sigma_{\mathcal{OO}} & \Sigma_{\mathcal{OU}} \\ \Sigma_{\mathcal{UO}} & \Sigma_{\mathcal{UU}} \end{pmatrix}$, where

$$\Sigma_{\mathcal{UU}} = \begin{pmatrix} \mathcal{K}(u_1, u_1) & \dots & \mathcal{K}(u_1, u_m) \\ \vdots & & \vdots \\ \mathcal{K}(u_m, u_1) & \dots & \mathcal{K}(u_m, u_m) \end{pmatrix} \tag{5}$$

in which $\mathcal{K}(u_i, u_j) = \mathcal{K}(u_i, u_j, \vec{d}_{ui}, \vec{d}_{uj}, \mathcal{O}_k)$, and

$$\Sigma_{\mathcal{UO}}^T = \Sigma_{\mathcal{OU}} = \begin{pmatrix} \mathcal{Q}(o_1, u_1) & \dots & \mathcal{Q}(o_1, u_m) \\ \vdots & & \vdots \\ \mathcal{Q}(o_n, u_1) & \dots & \mathcal{Q}(o_n, u_m) \end{pmatrix} \tag{6}$$

in which $\mathcal{Q}(o_j, u_i) = \mathcal{Q}(u_i, o_j, \vec{d}_{ui}, \vec{d}_{oj})$. Thus, to objects set $\mathcal{O}$ and UAV set $\mathcal{U}$, the conditional covariance is

$$\sigma^2_{\mathcal{O}|\mathcal{U}} = tr(\Sigma_{\mathcal{OO}}) - tr(\Sigma_{\mathcal{OU}} \Sigma^{-1}_{\mathcal{UU}} \Sigma_{\mathcal{UO}}). \tag{7}$$

where $tr(\cdot)$ is the *trace function* of a matrix.

C. Problem Formulation

First, as we seek to maximize the recognition accuracy, we need to minimize the variance of $\mathcal{O}$ given $\mathcal{U}$. Namely, we need to maximize the negation of the variance. As $tr(\Sigma) = tr(\Sigma_{\mathcal{OO}}) + tr(\Sigma_{\mathcal{UU}})$, we have

$$max \quad tr(\Sigma_{\mathcal{UU}}) + tr(\Sigma_{\mathcal{OU}} \Sigma^{-1}_{\mathcal{UU}} \Sigma_{\mathcal{UO}}). \tag{8}$$

Then, we define the overall monitoring utility as shown in Equation (8). Our task is to find the optimal strategies for all M UAVs to maximize the overall monitoring utility. Thus, the problem of placement of Unmanned Aerial VehIcles for aniSotropic monItoring Tasks (VISIT) is defined as follows:

$$\textbf{(P1)} \quad \begin{aligned} max \quad & tr(\Sigma_{\mathcal{UU}}) + tr(\Sigma_{\mathcal{OU}} \Sigma^{-1}_{\mathcal{UU}} \Sigma_{\mathcal{UO}}) \\ s.t. \quad & |U| = M. \end{aligned}$$

where $tr(\cdot)$ is the trace function of matrix, $\Sigma_{\mathcal{UU}}$ and $\Sigma_{\mathcal{OU}}$ are establish as Equation (5) and (6), and $\Sigma^{-1}_{\mathcal{UU}}$ is the inverse matrix of $\Sigma_{\mathcal{UU}}$. Consider the simple case in which $\omega = \beta = \gamma = \theta = 2\pi$, $D = 1$ and the QoM for any pair of UAV and object is the same. Then, VISIT is reduced to the well-known Unit Disk Coverage problem [26], which is known to be NP-hard. Thus, we have the following theorem. Note that we omit some theoretical proofs in this paper to save space.

***Theorem** 3.1:* The VISIT problem is NP-hard.

IV. Solution

In this section, we present an algorithm with approximation ratio $1 - 1/e - \epsilon$ to address VISIT, which consists of three steps. First, as QoM is nonlinear with distance and angle, we approximate the QoM by a piecewise constant function with distance and angle. By doing so, the monitoring region is divided into many subareas and the approximated QoM at any point in each subarea is constant. Then, we present a Monitoring Dominating Set extraction method to reduce the continuous search space of strategies of UAVs to a limited number of strategies without performance loss. Thereby, our problem is transformed into finding M strategies among the obtained strategies to maximize the overall monitoring utility. Finally, we prove that the transformed problem falls into the realm of maximizing a monotone submodular optimization problem subject to a uniform matroid constraint, and propose a greedy algorithm with performance guarantee.

A. Area Discretization

1) Piecewise Constant Approximation of QoM: Let $\mathcal{Q}(d, \alpha)$ denote the QoM of an object that is monitored by a UAV with distance d and angle α, *i.e.*, $\mathcal{Q}(d, \alpha) = \frac{a}{(d+b)^2} \cos \alpha$ where $0 \le d \le D, 0 \le \alpha \le \theta$, and $\mathcal{Q} = 0$ otherwise. We use multiple piecewise constant segments $\tilde{\mathcal{Q}}(d, \alpha)$ to approximate $\mathcal{Q}(d, \alpha)$ and bound both approximation error and computational cost.

Figure 5 depicts the key idea of the approximation method of $\mathcal{Q}(d, \alpha)$. Let $l(0), l(1), \cdots, l(K_1)$ be the end points in distance domain of K_1 constant segments which divides the sector model of objects into K_1 sector rings. Then, in each sector ring, *e.g.*, between $l(k)$ and $l(k+1)$, let $a(0), a(1), \cdots, a(K_2)$ be the end points in angle domain of constant segments, which divides each sector ring into $K_{2,k} = K_2$ segments both left and right of $\vec{d}_{oj}$. Thus, the sector of object is divided into $K = 2 \sum_{k=0}^{K_1 - 1} K_{2,k}$ number of segments. In Figure 5, K_1 is set to 2, $K_{2,0}$ and $K_{2,1}$ are set to 2 and 3 respectively.

***Definition** 4.1:* Setting $l(0) = 0$, $l(K_1) = D$, $a(0) = 0$ and $a(K_2) = \theta$, the piecewise constant QoM function $\tilde{\mathcal{K}}(d, \alpha)$ can be defined as:

$$\tilde{\mathcal{Q}}(d, \alpha) = \begin{cases} \mathcal{Q}(l(1), a(1)), & d = l(0), \alpha = a(0) \\ \mathcal{Q}(l(k), a(k)), & l(k-1) < d \le l(k), \\ & a(k-1) < \alpha \le a(k) \\ 0, & d > l(K_1), \alpha > \theta. \end{cases} \tag{9}$$

We bound the approximation error and the computational overhead by two steps. First, we regard α as a constant and bound the approximation error of $\mathcal{Q}(d, \alpha)$ to be less than ϵ_d in distance domain.

***Theorem** 4.1:* For any given $\alpha = c$, setting $l(0) = 0$, $l(K_1) = D$, and $l(k_1) = b((1 + \epsilon_d)^{k_1/2} - 1)$, ($k_1 = 1, \cdots, K_1 - 1$, and $K_1 = \lceil \frac{ln(\mathcal{Q}(0,\alpha)/\mathcal{Q}(D,\alpha))}{ln(1+\epsilon_d)} \rceil$), we have the approximation error:

$$1 \le \frac{\mathcal{Q}(d, c)}{\tilde{\mathcal{Q}}(d, c)} \le 1 + \epsilon_d, (d \le D). \tag{10}$$

Then, we bound the approximation error in each segment to be less than ϵ_1.

***Theorem** 4.2:* In each piecewise $l(k_1) \le d \le l(k_1 + 1)$, setting $a(0) = 0$, $a(K_2) = \theta$, and $a(k_2) = \arccos(\frac{1+\epsilon_d}{1+\epsilon_1})^{k_2}$, ($k_2 = 1, \cdots, K_2 - 1$, and $K_2 = \lceil \frac{ln(\mathcal{Q}(l(k_1),0)/(\mathcal{Q}(l(k_1+1),\theta)\cdot(1+\epsilon_d)))}{ln((1+\epsilon_1)/(1+\epsilon_d))} \rceil$), we have the approximation error:

$$1 \le \frac{\mathcal{Q}(d, \alpha)}{\tilde{\mathcal{Q}}(d, \alpha)} \le 1 + \epsilon_1, (d \le D, \alpha \le \theta). \tag{11}$$

Algorithm 1: MDS Extraction

Input: Subarea A_i and its candidate monitored set $\tilde{O}_i$
Output: MDSs and their corresponding strategies

for *all pairs of objects in* $\tilde{O}_i$*, say* o_i *and* o_j **do**
  Draw a straight line crossing o_i and o_j, which intersects with the boundaries of subarea.
  Place UAVs at these intersection points and adjust their orientations such that right radius of monitoring area crossing o_i and o_j.
  Add the obtained candidate MDSs and the corresponding strategies under current setting into the solution set.
  Draw two arcs crossing o_i and o_j with circumferential angle $2 \cdot \gamma$, which intersects the boundaries of subarea.
  Place UAVs at these intersection points and adjust their orientations such that the two radiuses cross o_i and o_j respectively.
  Add the obtained candidate MDSs and the corresponding strategies under current setting into the solution set.
Choose a point on the boundary of the subarea randomly and rotates the orientation of a UAV located at the point anticlockwise from 0 to 2π, and meanwhile, track and record the current set of monitoring objects.
Filter the solution set by removing those non-MDSs and their corresponding strategies.

2) Approximation for Fusion Function: By Theorem 4.1 and 4.2, approximation error in angle domain is bounded by $\frac{1+\epsilon_1}{1+\epsilon_d}$. So, the fusion function can be bounded as follows.

***Theorem** 4.3:* In each segment $a(i) \leq \alpha(\vec{d}_{ok}, \overrightarrow{o_k u_i}) \leq a(i+1)$ and $a(j) \leq \alpha(\vec{d}_{ok}, \overrightarrow{o_k u_j}) \leq a(j+1)$ in Equation (9), setting $\alpha(\vec{d}_{ok}, \overrightarrow{o_k u_i}) = a(i)$ and $\alpha(\vec{d}_{ok}, \overrightarrow{o_k u_i}) = a(j)$, then we have the following approximation error:

$$1 \leq \frac{\mathcal{K}(u_i, u_j, \vec{d}_{ui}, \vec{d}_{uj}, \mathcal{O}_k)}{\tilde{\mathcal{K}}(u_i, u_j, \vec{d}_{ui}, \vec{d}_{uj}, \mathcal{O}_k)} \leq \frac{1+\epsilon_1}{1+\epsilon_d}, (\alpha(\cdot) \leq \theta). \quad (12)$$

3) Discretizing Area: The key idea of area discretization is illustrated in Figure 6. First, we draw concentric sectors with radius $l(0), l(1), \cdots, l(K_1)$ and central angle θ centered at each object, respectively. Then, between each pair of adjacent concentric arcs $l(k_1)$ and $l(k_1+1)$, we draw line segments at each side of orientation of objects and their included angles with $\vec{d}_{oj}$ are $a(0), a(1), \cdots, a(K_2)$. By doing so, the monitored areas of objects are discretized and intersected with each other. Due to geometric symmetry, if a UAV is located between two concentric sectors with radius $l(k_1)$ and $l(k_1+1)$ with respect to an object, then the object must also lie between two sectors with the same radius centered at the UAV, leading to a constant approximated QoM if the UAV monitoring this object between line segments $a(k_2)$ and $a(k_2+1)$ of this object. In Figure 6, UAV u_1 locates between sectors with radius $l(0)$ and $l(1)$ centered at objects o_1 and o_2 as well as $l(1)$ and $l(2)$ centred at object o_3, and the approximated QoM of o_1 and o_3 by u_1 is $\mathcal{Q}(l(1), a(1))$ and $\mathcal{Q}(l(2), a(1))$. Moreover, we have the following theorem regarding the number of discretized subareas.

***Theorem** 4.4:* The number of discretized subareas for N objects is $O(N^2 \epsilon_d^{-2} \epsilon_1^{-2})$.

B. Monitoring Dominating Set (MDS) Extraction

After the area discretization, we only need to consider the relationship between objects and UAVs in each subarea. In this subsection, we show that we do not need to enumerate all possible covered set of objects, but just need to consider a limited number of representative monitored sets of objects, *i.e.*, Monitoring Dominating Sets (MDSs), and figure out these corresponding strategies. This idea borrowed from some previous work [16], [27]–[29]

1) Preliminaries: In the first place, we give the following definitions to assist analysis.

***Definition** 4.2:* **(Dominating Relation)** Given two strategies $\langle u_1, \vec{d}_{u1} \rangle$ and $\langle u_2, \vec{d}_{u2} \rangle$ and their monitored object sets O_1 and O_2. If $O_1 = O_2$, we say $\langle u_1, \vec{d}_{u1} \rangle$ is equivalent to $\langle u_2, \vec{d}_{u2} \rangle$; If $O_1 \supseteq O_2$, we say $\langle u_1, \vec{d}_{u1} \rangle$ dominates $\langle u_2, \vec{d}_{u2} \rangle$.

***Definition** 4.3:* **(Monitoring Dominating Set)** Given a set of objects O_i monitored by a strategy $\langle u_i, \vec{d}_{ui} \rangle$, if there does not exist any strategy $\langle u_j, \vec{d}_{uj} \rangle$ such that $\langle u_j, \vec{d}_{uj} \rangle$ dominates $\langle u_i, \vec{d}_{ui} \rangle$, then O_i is a maximum dominating set and we call it Monitoring Dominating Set (MDS).

Given a subarea, due to limited monitoring angle of field of view of UAVs, there may be only a few objects in the ground set of objects can be monitored by a UAV inside the subarea.

***Definition** 4.4:* **(Candidate Monitored Set)** The candidate monitored set $\tilde{O}_i$ for subarea A_k is the set of objects can be monitored by a UAV u_i with some orientation $\vec{d}_{ui}$ in A_k.

Obviously, any MDS of a subarea must belong to the subarea's candidate monitored set $\tilde{O}_i$. As placing UAVs for monitoring MDSs is always better than for monitoring MDSs' subsets, we focus on finding all MDSs and their strategies.

2) MDS Extraction: We first give an example for illustration of Algorithm 1. As shown in Figure 7(a), there are six objects in the candidate monitored set of objects of subarea A_i. First, we draw lines crossing each pair of objects, *e.g.*, o_1 and o_2 in Figure 7(b), and place a UAV at intersection points u_1 and u_2 with two objects lying on its clockwise boundary, then we obtain two MDSs $\{o_1, o_2, o_4\}$, $\{o_1, o_2, o_4, o_5, o_6\}$ and their strategies $\langle u_1, \vec{d}_{u1} \rangle$, $\langle u_2, \vec{d}_{u1} \rangle$. Second, we draw arcs crossing each pair of objects with circumferential angle $2 \cdot \gamma$, *e.g.*, o_1 and o_5 in Figure 7(c), and place a UAV at intersection points u_3 and u_4 with two objects on its two radiuses, respectively. Then we obtain two MDSs $\{o_1, o_2, o_4, o_5\}$ of $\langle u_3, \vec{d}_{u2} \rangle$ and $\{o_1, o_4, o_5\}$ of $\langle u_4, \vec{d}_{u3} \rangle$. Third, we randomly choose a point on the boundary of subarea and anticlockwise rotate orientation of a UAV located at the point subarea from 0 to 2π, as shown in Figure 7(d). During the process, it tracks the current set of monitoring objects, and records all MDSs. Finally, we check all the obtained MDSs and remove smaller MDSs then reserve $\{o_1, o_2, o_4, o_5, o_6\}$.

Now, we prove the correctness of this algorithm of MDS extraction. To begin with, we give three transformations to assist our proof. All of them are transformed from strategy $\langle u_1, \vec{d}_{u1} \rangle$ as shown in Figure 8. *Rotation* transformation keeps the coordinate of UAV u_i unchanged and rotates the orien-

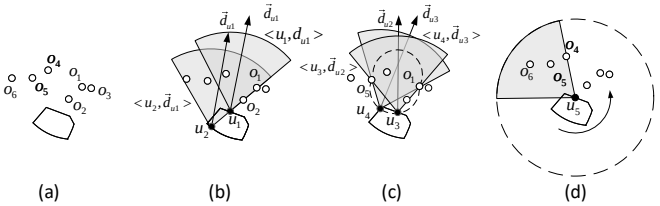

Fig. 7: An example of MDS extraction

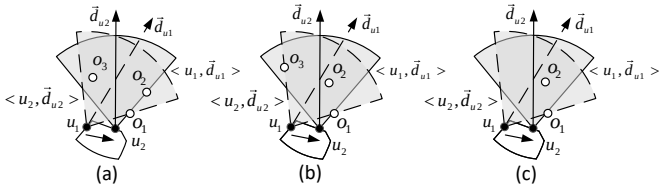

Fig. 9: Three critical conditions of transformation

Algorithm 2: Strategy Selection

Input: The number of UAVs M, MDS set Γ, object function $f(X)$

Output: Strategy set X

1 $X = \emptyset$.
2 **while** $|X| \leq M$ **do**
3 $\quad e^* = \arg\max_{e \in \Gamma \setminus X} f(X \cup \{e\}) - f(X)$.
4 $\quad X = X \cup \{e^*\}$.

tation of UAV from $\vec{d}_{u1}$ to $\vec{d}_{u2}$. *Translation* transformation keeps the orientation of UAV $(\vec{d})_{ui}$ unchanged and moves the coordinate of UAV from u_1 to u_2. *Projection* transformation is a special case of translation transformation. It keeps the orientation unchanged and moves the coordinate of UAV along the reverse direction of orientation $\vec{d}_{u1}$ until reaching some point u_2 on the boundary of the subarea.

According to the transformation of projection, we have the following lemma. We omit the proof to save space.

Lemma 4.1: If $\langle u_2, \vec{d}_{u1} \rangle$ is the projection of $\langle u_1, \vec{d}_{u1} \rangle$, then $\langle u_2, \vec{d}_{u1} \rangle$ dominates $\langle u_1, \vec{d}_{u1} \rangle$.

By Lemma 4.1, we can get the following corollary.

Corollary 4.1: The MDSs extracted under the case of UAVs on the boundaries of a subarea dominate the MDSs extracted under the case of UAVs in the whole subarea.

Thus, we only need to consider the strategies $\langle u_i, \vec{d}_{ui} \rangle$ where u_i located on the boundaries of the subarea. Let Γ denote the output set of Algorithm 1. We have the following theorem.

Theorem 4.5: Given any strategy $\langle u, \vec{d}_u \rangle$, there exists $\langle u_2, \vec{d}_{u2} \rangle \in \Gamma$ such that $\langle u_2, \vec{d}_{u2} \rangle$ dominates $\langle u, \vec{d}_u \rangle$.

Proof: As per Corollary 4.1, we only need to consider the strategies of coordinates on the boundaries of the subarea. For an arbitrary strategy $\langle u, \vec{d}_u \rangle$, we execute the following transformations. **(1)** Keep the coordinate u fixed and rotate the orientation $\vec{d}_u$ anticlockwise, *i.e.*, rotation transformation, until there is at least one object, saying o_1, going to fall out of monitoring area through the right radius. Suppose the obtained strategy is $\langle u_1, \vec{d}_{u1} \rangle$, where $u_1 = u$. Obviously, $\langle u_1, \vec{d}_{u1} \rangle$ dominates $\langle u, \vec{d}_u \rangle$. **(2)** Keep the right radius of the UAV's monitoring area crossing o_1 and move the UAV along the

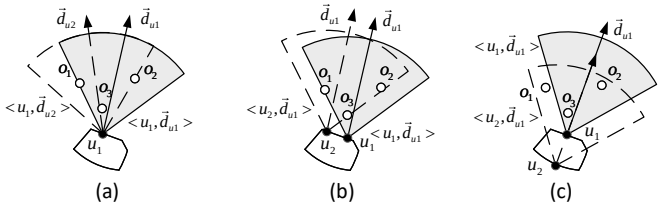

Fig. 8: Three kinds of transformation: (a) Rotation, (b) Translation, (c) Projection

boundaries of subarea, until at least another object is going to fall out through either right or left radius. Suppose the obtained strategy is $\langle u_2, \vec{d}_{u2} \rangle$. If no other object is going to fall out, then stop the transformation. During the transformations, any object monitored currently won't fall out of the monitoring area, which means $\langle u_2, \vec{d}_{u2} \rangle$ dominates $\langle u_1, \vec{d}_{u1} \rangle$.

After the above transformations, there are three possible cases we may encounter. **Case 1:** Another object touches the right radius of the monitoring area (Figure 9(a)). **Case 2:** Another object touches the left radius of the monitoring area (Figure 9(b)). **Case 3:** None of other object touches the boundary of the monitoring area (Figure 9(c)). Case 1 and 2 are critical conditions that an object which is monitored by $\langle u_1, \vec{d}_{u1} \rangle$ is going to fall out the monitoring area. While Case 3 is the situation that objects never fall out, formally $\langle u_2, \vec{d}_{u2} \rangle$ is always equivalent to $\langle u_1, \vec{d}_{u1} \rangle$. In Algorithm 1, Step 2-4 and Step 5-7 correspond to Case 1 and 2, respectively. For Case 3, all points on the boundaries of subarea are equivalent, thus Step 8 can extract all MDSs resulted from this case. Consequently, the corresponding monitored set of objects of strategy $\langle u_2, \vec{d}_{u2} \rangle$ must be included in Γ before Step 9. Since it is dominated by some MDS in the final obtained Γ, the result follows. ■

C. Problem Reformulation and Solution

In this subsection, we show how to select a given number of strategies from the above obtained ones to maximize the overall monitoring utility. We first reformulate the problem, then prove its monotonicity and submodularity, and finally present an effective algorithm to address this problem.

Let $\mathcal{S}$ be the selected set of strategies from Γ. For all possible $\mathcal{S}$ in Γ, we can compute their overall monitoring utility. The problem **P1** can be reformulated as

$$\textbf{(P2)} \quad \begin{aligned} max \quad & tr(\Sigma_{\mathcal{SS}}) + tr(\Sigma_{\mathcal{OS}} \Sigma_{\mathcal{SS}}^{-1} \Sigma_{\mathcal{SO}}) \\ s.t. \quad & \mathcal{S} \subseteq \Gamma, |\mathcal{S}| = M, \end{aligned}$$

where $\Sigma_{\mathcal{OS}}$ and $\Sigma_{\mathcal{SS}}^{-1}$ can be easily obtained by Equation (9) with corresponding o_i and $s_i = \langle u_i, \vec{d}_{ui} \rangle$ and Equation (12) with s_i and s_j and their monitoring objects set $\mathcal{O}_i$ and $\mathcal{O}_j$.

The problem is then transformed to a combinatorial optimization problem. Now, we give the following definitions to assist further analysis before addressing **P2**.

Definition 4.5: [30] Let S be a finite ground set. A real-valued set function $f : 2^S \to \mathbb{R}$ is normalized, monotonic, and submodular if and only if it satisfies the following conditions, respectively: (1) $f(\emptyset) = 0$; (2) $f(A \cup \{e\}) - f(A) \geq 0$ for any $A \subseteq S$ and $e \in S \backslash A$; (3) $f(A \cup \{e\}) - f(A) \geq f(B \cup \{e\}) - f(B)$ for any $A \subseteq B \subseteq S$ and $e \in S \backslash B$.

***Definition** 4.6:* [30] A Matroid $\mathcal{M}$ is a strategy $\mathcal{M} = (S, L)$ where S is a finite ground set, $L \subseteq 2^S$ is a collection of independent sets, such that (1) $\emptyset \in L$; (2) if $X \subseteq Y \in L$, then $X \in L$; (3) if $X, Y \in L$, and $|X| < |Y|$, then $\exists y \in Y \backslash X$, $X \cup \{y\} \in L$.

***Definition** 4.7:* [30] Given a finite set S and an integer k. A uniform matroid $\mathcal{M} = (S, L)$ is a matroid where $L = \{X \subseteq S : |X| \leq k\}$.

Then, our problem can be reformulated as

$$\textbf{(P3)} \quad \begin{aligned} max\ & f(X) = tr(\Sigma_{XX}) + tr(\Sigma_{\mathcal{O}X}\Sigma_{XX}^{-1}\Sigma_{X\mathcal{O}}), \\ s.t.\ & X \in L, \\ & L = \{X \subseteq \Gamma : |X| \leq \mathcal{M}\}. \end{aligned}$$

***Lemma** 4.2:* The objective function $f(X)$ in **P3** is monotone submodular while its constraint is a uniform matroid one.

Proof: We verify the three listed requirements in Definition 4.5. First, when the number of UAVs is 0, obviously $\Sigma = 0$, thus $f(\emptyset) = 0$. Next, we present the following claim.

***Claim** 4.1:* Given a *semi-positive definite (s.p.d.)* matrix Σ in a block separated form as

$$\Sigma = \begin{pmatrix} A & E & F & G \\ E^T & B & H & I \\ F^T & H^T & C & J \\ G^T & I^T & J^T & D \end{pmatrix},$$

1. $tr(A) + tr((EFG)(EFG)^T A^{-1})$
$$\leq tr(A+B) + tr(\begin{pmatrix} F & G \\ H & I \end{pmatrix}\begin{pmatrix} F & G \\ H & I \end{pmatrix}^T \begin{pmatrix} A & E \\ E^T & B \end{pmatrix}^{-1}), \quad (13)$$

2. $tr(A+B) + tr(\begin{pmatrix} F & G \\ H & I \end{pmatrix}\begin{pmatrix} F & G \\ H & I \end{pmatrix}^T \begin{pmatrix} A & E \\ E^T & B \end{pmatrix}^{-1})$
$$- (tr(A) + tr(EFG)(EFG)^T A^{-1}) \leq$$
$$tr(A+B+C) + tr(\begin{pmatrix} G \\ I \\ J \end{pmatrix}\begin{pmatrix} G \\ I \\ J \end{pmatrix}^T \begin{pmatrix} A & E & F \\ E^T & B & H \\ F^T & H^T & C \end{pmatrix}^{-1})$$
$$- (tr(A+C) + tr(\begin{pmatrix} G \\ J \end{pmatrix}\begin{pmatrix} G \\ J \end{pmatrix}^T \begin{pmatrix} A & F \\ F^T & C \end{pmatrix}^{-1})). \quad (14)$$

Proof: For Inequation (13), we set $M = (FG)$,

$$\begin{pmatrix} M \\ N \end{pmatrix} = \begin{pmatrix} F & G \\ H & I \end{pmatrix}, \begin{pmatrix} O & P \\ P^T & Q \end{pmatrix} = \begin{pmatrix} A & E \\ E^T & B \end{pmatrix}^{-1}.$$

Then, expanding (13) and combining like terms, we get $tr(A+E^TA^{-1}E)+tr(M^TA^{-1}M) \leq tr(A+B)+tr(M^TOM+N^TP^TM+M^TPN+N^TQN$. Now, we prove it by two parts.

(1) $tr(A + E^TA^{-1}E) \leq tr(A + B)$: As Σ is an *s.p.d.* matrix, for any real vectors x and y, we have $(x, y)^T \begin{pmatrix} A & E \\ E^T & B \end{pmatrix} (x, y) > 0$. As an *s.p.d.* matrix can always be factorized as a matrix times its transpose, we can rewrite the left of (13) as $x^TR^TRx + x^TR^TR^{-T}Ey + y^TE^TR^{-1}Rx + y^TBy + y^TE^TR^{-1}R^{-T}Ey - y^TE^TA^{-1}Ey$, where R is invertible and $R^{-T} = (R^T)^{-1}$. Thus, (13) can be rewritten as $(Rx + R^TEy)^T(Rx + R^{-T}Ey) + y^T(-E^TA^{-1}E + B)y > 0$. As A is *s.p.d.*, $Ax + Ey = 0$ with respect to x always has a solution for any y, then vector $(Rx + R^TEy)$ equals to 0 for any given y. That means, for any given y, there always exists $y^T(-E^TA^{-1}E+B)y > 0$. So, $(-E^TA^{-1}E+B)$ is *s.p.d.*, which implies $tr(-E^TA^{-1}E+B) > 0$ and then $tr(E^TA^{-1}E) < tr(B)$.

(2) $tr(M^TA^{-1}M) \leq tr(M^TOM + N^TP^TM + M^TPN + N^TQN)$: Let the right of the inequality minus the left, we need to prove $tr(\Phi) \geq 0$, $\Phi = M^T(O-A^{-1})M+N^TP^TM+M^TPN+N^TQN$. Because $AO + EP^T = I$ and $AP + EQ = 0$, which implies $O + A^{-1}EP^T = A^{-1}$ and $PQ^{-1}P^T + A^{-1}EP^T = 0$, then we have $M^T(O - A^{-1})M = M^T(PQ^{-1}P^T)M$. Then $\Phi = M^T(PQ^{-1}P^T)M + N^TP^TM + M^TPN + N^TQN$, which leads to

$$(M^TN^T)\begin{pmatrix} P & 0 \\ Q & I \end{pmatrix}\begin{pmatrix} Q^{-1} & 0 \\ 0 & 0 \end{pmatrix}\begin{pmatrix} P & Q^T \\ 0 & I \end{pmatrix}(MN)^T.$$

As Q^{-1} is *s.p.d.*, the result follows. Combine the above two parts, the whole result follows. ■

By Inequation (13), we obtain $f(A \cup \{e\}) - f(A) \geq 0$, where, $A \subseteq \Gamma$ and element $e \in \Gamma \backslash A$. And according to (14), we have $(f(A \cup \{e\}) - f(A)) - (f(B \cup \{e\}) - f(B)) \geq 0$, where A and B are two sets such that $A \subseteq B \subseteq \Gamma$ and element $e \in \Gamma \backslash B$. We omit the proof of Inequation (14) as it is similar to that of Inequation (13).

To sum up, $f(X)$ is a monotone submodular function. Moreover, we omit the proof for the characteristic of the constraint in **P3** to save space. ■

Consequently, the reformulated problem falls into the scope of maximizing a monotone submodular function subject to a matroid constraint, which can be addressed by a greedy algorithm which achieves a constant approximation ratio [30]. Algorithm 2 shows the pseudo code of strategy selecting algorithm. In each round, Algorithm 2 greedily adds a strategy e^* to X to maximize the increment of function $f(X)$.

***Theorem** 4.6:* The VISIT algorithm achieves an approximation ratio of $1 - \frac{1}{e} - \epsilon$, where $\epsilon = 3\epsilon_1$, and its time complexity is $O(MN^{12}\epsilon^{-12})$.

V. Simulation Results

A. Evaluation setup

In our simulation, objects are uniformly distributed in a $10\,m \times 10\,m$ 2D square area and their orientations are randomly selected among $[0, 2\pi]$. If no otherwise stated, we set $N = 12$, $M = 9$, $\gamma = \pi/3$, $\theta = \pi/6$, $D = 3\,m$, $\omega = \pi/18$, $\beta = \pi/3$, $\epsilon = 0.2$, and $\epsilon_d = \sqrt{\epsilon/3}$, respectively. We also simulate the coordinates of UAVs which follow a 2D Gaussian distribution with both x- and y- coordinate randomly selected from a Gaussian distribution with $\mu = u_i$ and $\sigma_x = \sigma_y = 3$. Each data point in figures is computed by averaging results of 200 random topologies and normalized by dividing the best total QoM. As there are no existing methods for VISIT, we present three algorithms for comparison: (1) Grid Coordinate Monitoring Algorithm (GCMA) first divides whole 2D square area into small grids with $D/\sqrt{2}\,m$ side length, then extracts MDSs at each vertex of grids like Algorithm 1 does in line 8, and finally greedily selects the strategies with the most number of objects. (2) Number-Objective Monitoring

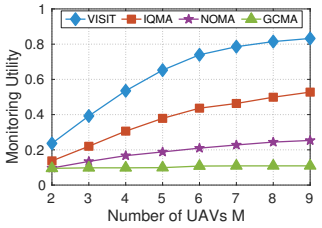

Fig. 10: M vs. utility

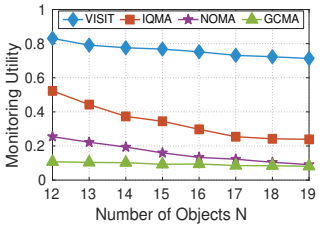

Fig. 11: N vs. utility

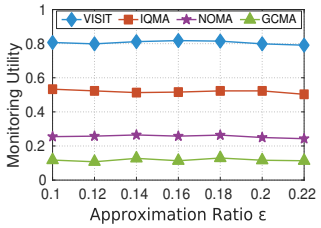

Fig. 12: ϵ vs. utility

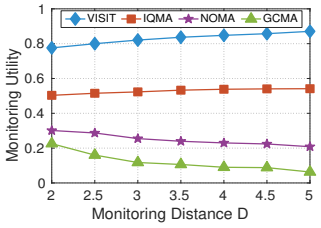

Fig. 13: D vs. utility

TABLE II: Coordinates and orientations of objects

Object	Coordinate (m)	Orientation
o_0	(4.32, 11.58)	234.21°
o_1	(11.93, 3.22)	114.43°
o_2	(9.94, 14.34)	256.84°
o_3	(2.44, 3.75)	133.28°
o_4	(4.40, 13.43)	294.20°
o_5	(12.50, 0.73)	103.95°
o_6	(5.56, 12.53)	168.34°
o_7	(7.62, 0.45)	240.33°
o_8	(3.55, 4.71)	197.91°
o_9	(7.09, 3.16)	282.47°
o_{10}	(3.97, 0.44)	69.88°
o_{11}	(8.97, 5.60)	194.79°
o_{12}	(10.32, 6.08)	341.20°
o_{13}	(3.28, 4.12)	114.87°
o_{14}	(8.87, 14.05)	278.88°

Algorithm (NOMA) divides the area with the intersection of monitoring sectors and extracting MDSs with MDS extraction algorithm. (3) Isotropic-QoM Monitoring Algorithm (IQMA) improves NOMA by introducing QoM which is influenced by the distance between object and UAV, but the QoM is isotropic.

B. Performance Comparison

1) Impact of Number of UAVs M: Our simulation results show that on average, VISIT outperforms IQMA, NOMA, and GCMA by 68.03%, 2.28 *times, and* 5.05 *times, respectively, in terms of* M. Figure 10 shows that the monitoring utility of VISIT invariably increases with M until it approaches 1, while that of IQMA and NOMA increase to about 0.58 and 0.22, respectively. However, due to the limited candidate coordinate of UAVs, GCMA always remains low.

2) Impact of Number of Objects N: Our simulation results show that on average,VISIT outperforms IQMA, NOMA, and GCMA by 1.24 *times,* 3.74 *times, and* 7.11 *times, respectively, in terms of* N. Figure 11 shows that the monitoring utility decreases monotonically as the number of objects increases for all the four algorithms. Particularly, both the monitoring utilities of GCMA decrease more slowly than that of VISIT, IQMA, and NOMA, because VISIT, IQMA, and NOMA select positions that can generate more utility, but GCMA cannot.

3) Impact of Efficient Angle ϵ: Our simulation results show that on average, VISIT outperforms IQMA, NOMA, and GCMA by 55.18%, 2.15 *times, and* 5.83 *times, respectively, in terms of* ϵ. As shown in Figure 12, the monitoring utility of VISIT fluctuates slightly when ϵ grows, but it is almost always larger than 0.8. This provides us with a good opportunity to select a larger ϵ to reduce the computation overhead of VISIT without noticeable degradation of performance.

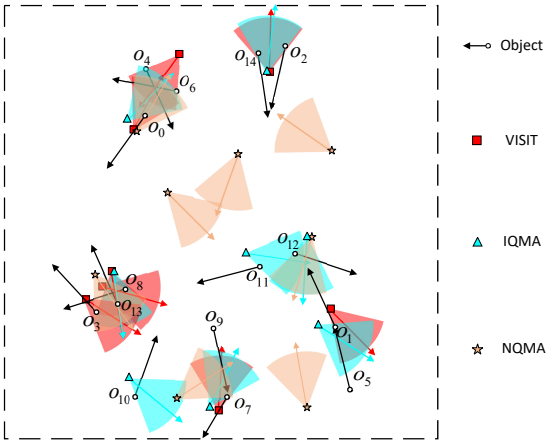

Fig. 14: Objects distribution and UAV placement of VISIT, IQMA, and NOMA

4) Impact of Farthest Sight Distance D: Our simulation results show that on average, VISIT outperforms IQMA, NOMA, and GCMA by 57.25%, 2.33 *times, and* 5.83 *times, respectively, in terms of* D. Figure 13 shows that the monitoring utility of VISIT monotonically increases with D until it approaches 1.The monitoring utility of NOMA decreases because it only maximizes the number of monitoring objects, and that of GCMA decreases because the side length of grids decreases when D increases.

VI. Field Experiments

In this section, we conduct field experiments. As shown in Figure 15, our experiments involve a few DJI Phantom 4 advanced UAVs and 15 objects. In our experiment, 15 objects are uniform random distributed in a $15\,m \times 15\,m$ experimental field, and the coordinate and orientation of objects are shown in Table II. Figure 14 illustrates the distribution of 15 objects and the strategies of 7 UAVs of VISIT, IQMA, and NOMA with red, blue, and yellow sectors, respectively. we use 15 objects as shown in Figure 15. Each of them is a semicircle cylinder that has an $A4$ sheet of paper with different printed text, such as "ACDE3F", "ACDE8F", and "ACBE3F", pasted on it. Figure 18 shows the experimental field. Based on the hardware parameters of UAV and the size of semicircle cylinder, we set $\gamma = \pi/6$, $D = 7\,m$, $\omega = \pi/18$, $\beta = 4\pi/5$, and $\theta = 2\pi/5$,$\epsilon = 0.2$ and $\epsilon_d = \sqrt{\epsilon/3}$. Also, we add 35 other similar texts into candidate set of recognition results. We use the decision fusion model proposed in [31] as our fusion function and respectively feed 8 obtained figures of VISIT, IQMA, and NOMA to the text recognition approach proposed in [32]. As illustrated in Figure 16, the recognition

(a) UAV

(b) Text Object

Fig. 15: UAV & Objects

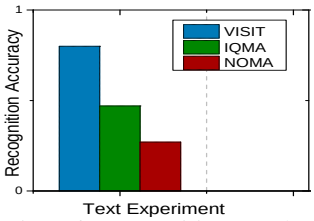

Fig. 16: Recognition results

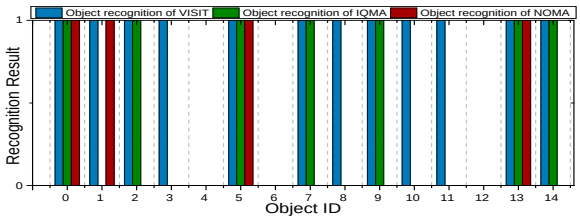

Fig. 17: Text object recognition

Fig. 18: Text experimental field

accuracy of VISIT outperforms IQMA and NOMA by 41.3% and 66.3%, respectively. Specifically, Figure 17 depicts the recognition results of each object, where 1 denotes the text object is successfully recognized while 0 denotes not.

VII. Conclusion

In this paper, we have studied the problem of placement of Unmanned Aerial Vehicles for anisotropic monitoring tasks. The key novelty of this paper is on proposing the first algorithm for UAV placement while considering anisotropic quality of monitoring. The key contributions of this paper are as follows. First, we established the anisotropic monitoring model which can be reused in other monitoring situations. Second, we developed an approximation algorithm with performance guarantee. Third, we conducted simulation and field experiments for evaluation. The key technical depth of this paper is in reducing the infinite solution space of this optimization problem to a limited one by utilizing the techniques of area partition and Monitoring Dominating Set extraction, and modeling the reformulated problem as maximizing a monotone submodular function subject to a matroid constraint. Our evaluation results show that our framework outperforms other comparison algorithms by at least 41.3%.

Acknowledgment

This work was supported in part by the National Key R&D Program of China under Grant No. 2018YFB1004704, in part by the National Natural Science Foundation of China under Grant No. 61502229, 61872178, 61832005, 61672276, 61472445, 61631020, 61702525, 61702545, 61872173, and 61321491, in part by the Natural Science Foundation of Jiangsu Province under Grant No. BK20181251, in part by the Fundamental Research Funds for the Central Universities under Grant 021014380079, in part by the Natural Science Foundation of Jiangsu Province under Grant No. BK20140076.5, in part by the Nature Science Foundation of Jiangsu for Distinguished Young Scientist under Grant BK20170039.

References

[1] S. He *et al.*, "Full-view area coverage in camera sensor networks: Dimension reduction and near-optimal solutions," *IEEE Transactions on Vehicular Technology*, 2016.

[2] S. Hayat *et al.*, "Survey on unmanned aerial vehicle networks for civil applications: A communications viewpoint," *IEEE Communications Surveys & Tutorials*, 2016.

[3] X. Liu *et al.*, "Optimizing trajectory of unmanned aerial vehicles for efficient data acquisition: A matrix completion approach," 2019.

[4] L. Hu *et al.*, "Uavs joint vehicles as data mules for fast codes dissemination for edge networking in smart city," in *Peer-to-Peer Networking and Applications*, 2019.

[5] "https://www.dji.com/phantom-4-adv/info."

[6] M. Kan *et al.*, "Multi-view deep network for cross-view classification," in *IEEE CVPR*, 2016.

[7] V. Blanz *et al.*, "Face recognition based on frontal views generated from non-frontal images," in *IEEE CVPR*, 2005.

[8] "https://www.dji.com/phantom-4-adv/info#specs."

[9] S. Tang *et al.*, "Morello: A quality-of-monitoring oriented sensing scheduling protocol in sensor networks," in *IEEE INFOCOM*, 2012.

[10] ——, "DAMson: On distributed sensing scheduling to achieve high quality of monitoring," in *IEEE INFOCOM*, 2013.

[11] Y. Wang *et al.*, "On full-view coverage in camera sensor networks," in *IEEE INFOCOM*, 2011.

[12] Y. Hu *et al.*, "Critical sensing range for mobile heterogeneous camera sensor networks," in *IEEE INFOCOM*, 2014.

[13] Y. Wang *et al.*, "Barrier coverage in camera sensor networks," in *ACM MobiHoc*, 2011.

[14] H. Ma *et al.*, "Minimum camera barrier coverage in wireless camera sensor networks," in *IEEE INFOCOM*, 2012.

[15] Z. Yu *et al.*, "Local face-view barrier coverage in camera sensor networks," in *IEEE INFOCOM*, 2015.

[16] W. Wang *et al.*, "PANDA: Placement of unmanned aerial vehicles achieving 3d directional coverage," in *IEEE INFOCOM*, 2019.

[17] E. Onur *et al.*, "How many sensors for an acceptable breach detection probability?" *Elsevier Comput. Commun.*, 2006.

[18] G. Xing *et al.*, "Data fusion improves the coverage of wireless sensor networks," in *ACM MobiHoc*, 2009.

[19] Q. Yang *et al.*, "Energy-efficient probabilistic area coverage in wireless sensor networks," *IEEE Transactions on Vehicular Technology*, 2015.

[20] J. Tao *et al.*, "A quality-enhancing coverage scheme for camera sensor networks," in *IEEE IECON*, 2017.

[21] A. Saeed *et al.*, "Argus: realistic target coverage by drones," in *ACM IPSN*, 2017.

[22] Z. Wang *et al.*, "Achieving k-barrier coverage in hybrid directional sensor networks," *IEEE Transactions on Mobile Computing*, 2014.

[23] G. Carlos *et al.*, "Near-optimal sensor placements in gaussian processes," in *ACM ICML*, 2005.

[24] A. Krause *et al.*, "Near-optimal sensor placements: maximizing information while minimizing communication cost," in *ACM IPSN*, 2006.

[25] T. Cover *et al.*, *Elements of information theory*. Wiley, 1991.

[26] R. G. Michael *et al.*, "Computers and intractability: a guide to the theory of np-completeness," *WH Free. Co., San Fr*, 1979.

[27] X. Wang *et al.*, "Heterogeneous wireless charger placement with obstacles," 2019.

[28] H. Dai *et al.*, "Optimizing wireless charger placement for directional charging," in *IEEE INFOCOM*, 2017.

[29] ——, "Wireless charger placement for directional charging," in *IEEE TON*, 2018.

[30] S. Fujishige, *Submodular functions and optimization*. Elsevier, 2005.

[31] R. Tan *et al.*, "Exploiting data fusion to improve the coverage of wireless sensor networks," *IEEE/ACM Transactions on Networking*, 2012.

[32] "https://github.com/yestinsong/text-detection."